

Synthesis and Evaluation of 8-halogenated-7-deaza-2'-deoxy-guanosine as 8-oxo-2'-deoxy-guanosine analogues

尹, 貽貞

<https://hdl.handle.net/2324/1500653>

出版情報：九州大学, 2014, 博士（創薬科学）, 課程博士
バージョン：
権利関係：やむを得ない事由により本文ファイル非公開（2）

【Introduction】

8-Oxo-2'-deoxyguanosine (8-oxo-dG) is a representative nucleoside damage that is formed by oxidation of 2'-deoxyguanosine (dG) with reactive oxygen species (ROS), and its presence has been linked to aging, cancer, etc [1]. Unlike dG, 8-oxo-dG forms stable base pairs with both 2'-deoxycytidine (dC) and 2'-deoxyadenosine (dA). Based on the base-pairing properties of 8-oxo-dG, DNA polymerases incorporate 8-oxo-dGTP opposite dA and dATP opposite 8-oxo-dG, causing AT to CG and GC to TA transversion mutations. To suppress the genotoxicity of 8-oxo-dG and protect the genome integrity, hOGG1 can excise 8-oxo-dG from 8-oxo-dG:dC base pairs within duplex DNA. And hMYH provides the defense by removing dA opposite 8-oxo-dG. To prevent the incorporation of 8-oxo-dGTP into DNA, hMTH1 hydrolyzes 8-oxo-dGTP to 8-oxo-dGMP that is further hydrolyzed by nucleotidase (Figure 1).

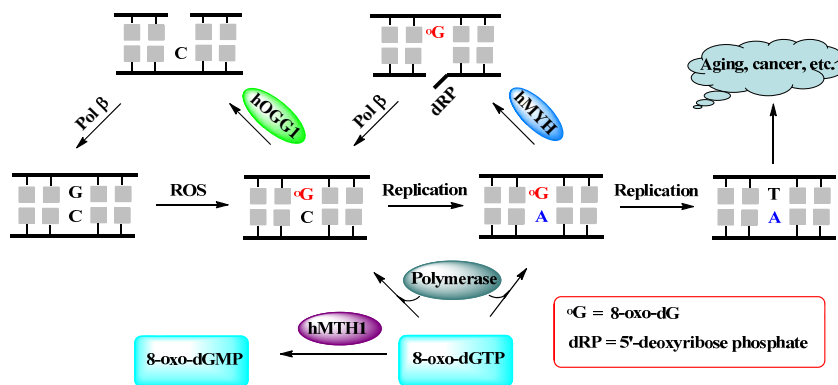


Figure 1. Mutation and repair of 8-oxo-dG

Recently, some DNA repair enzymes such as DNA polymerase β and hOGG1 have been regarded as antitumor targets. Especially, hMTH1 is responsible for removing of oxidized nucleotides and required for survival of cancer cells [2]. 8-Halogenated-7-deaza-dG derivatives were designed as 8-oxo-dG analogues to elucidate the contributions of N7-H and C8-oxygen to the base pairing, replication and repair of 8-oxo-dG. In this study, I have attempted to find out functional inhibitors of DNA repair enzymes among the 8-halogenated-7-deaza-dG derivatives (Figure 2).

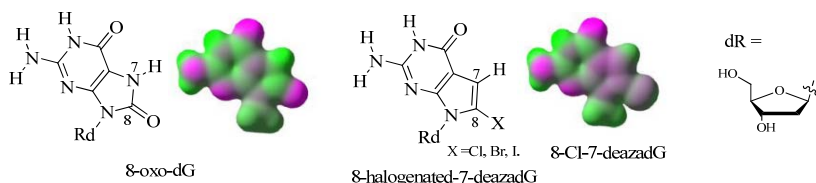
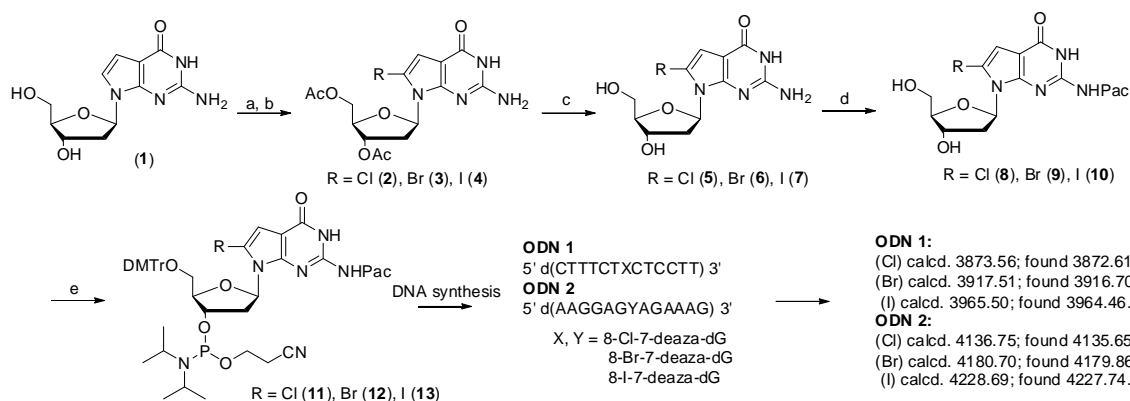


Figure 2. Structures of 8-oxo-dG and 8-halogenated-7-deazadG derivatives

【Experiments and Results】

1. Synthesis and base pairing properties of 8-halogenated-7-deaza-dG derivatives.

The syntheses of 8-halogenated-7-deaza-dG derivatives were achieved via the reaction between acetylated 7-deaza-dG and *N*-halogenated succinimides. These compounds were incorporated into the central part of 13-mer oligonucleotides (Scheme 1). The properties of these derivatives were investigated by computational, NMR and thermal denaturing studies. The significant upfield shift of the C-2' signals and characteristic downfield shift of H-2' signals indicated that 8-halogenated-7-deaza-dG derivatives prefer *syn*-conformation in DMSO solution similarly to 8-oxo-dG (Table 1). It was shown that the base pair of 8-halogenated-7-deaza-dG with dC was destabilized compared with dG, supporting their preference for *syn* conformation. Unlike 8-oxo-dG, 8-halogenated-7-deaza-dG did not form a stable base pair with dA, most likely due to the lack of N7-H hydrogen bonding with dA (Table 2 and Figure 3). Therefore, the newly-designed 8-halogenated-7-deaza-dG derivatives resemble 8-oxo-dG in shape and preference for *syn* conformation, but they do not form Hoogsteen base pair with the opposite dA.



Scheme 1. Reagents and conditions: (a) acetic anhydride, pyridine, 88%. (b) NRS (R = Cl, Br and I), DMF, 86%, 51% and 21%, respectively. (c) 7N ammonia in MeOH, 60-70%. (d) TMSCl, pyridine, followed by phenoxyacetic anhydride, pyridine, 70-80%. (e) (1) DMTrCl, pyridine. (2) 2-cyanoethyl-N,N'-diisopropyl-chlorophosphoroamidite, DIPEA, CH₂Cl₂, 39-61% over two steps.

Table 1. Selected chemical shift of corresponding diol compounds^a

Nucleoside	C1'	C2'	H2'	C8
dG	82.5	39.5	2.49	135.2
8-oxodG	81.2	35.7	2.96	151.6
deazadG	82.2	39.2	2.30	116.7
Cl-deazadG (5)	83.0	37.2	2.99	115.0
Br-deazadG (6)	84.2	37.3	3.04	101.9
I-deazadG (7)	86.8	37.5	3.12	71.3

^a ¹H and ¹³C NMR shifts were recorded using 0.04 M corresponding diol compounds in DMSO-d₆.

Table 2. Melting temperatures for the duplexes containing 8-halogenated-7-deaza-dG^a

Y	X			
	dC	dA	dG	dT
dG	44.1	35.4	35.7	33.7
8-oxodG	42.3	39.2	33.4	32.2
deazadG	41.6	35.4	32.0	33.1
Cl-deazadG (5)	38.0	30.3	31.4	30.8
Br-deazadG (6)	37.0	30.1	31.0	30.5
I-deazadG (7)	35.3	29.4	31.4	29.3

^a Conditions: 2 μM duplex, 100 mM NaCl and 10 mM sodium phosphate buffer, pH 7.0.

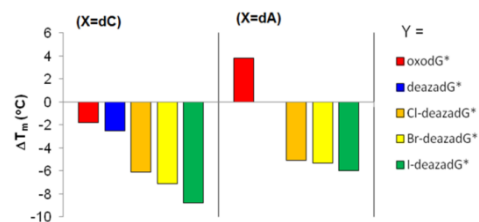


Figure 3. The bar graphs for the ΔT_m values between the corresponding dG analogues and dG in 2 μM solutions of duplex DNA. ($\Delta T_m(Z) = T_m(Z) - T_m(dG)$, Z represents modified dG).

2. Recognition and excision of 8-halogenated-7-deazadG in DNA duplex by 8-oxo-dG glycosidase.

I next tested the recognition and excision of 8-halogenated-7-deazadG derivatives in DNA duplex by Fpg and hOGG1. After incubation of the DNA duplex containing 8-oxo-dG analogues with Fpg and hOGG1 at 37°C, β-elimination and δ-elimination products are obtained which can be reflected on the gel (Figure 4). 8-Halogenated-7-deazadG derivatives, especially 8-Cl-7-deazadG, were good glycosidase substrates for Fpg. However, 8-halogenated-7-deazadG derivatives were slightly excised by hOGG1. Quartz crystal microbalance (QCM) provided the direct observation of the time courses of interaction between 8-halogenated-7-deazadG containing duplex and Fpg or hOGG1 (Figure 5 and Table 3). In the case of Fpg, the association rate constant (k_{on}) for dG or 7-deaza-dG was smaller than that for 8-oxo-dG and 8-halogenated-7-deazadG, suggesting that introducing C8-oxygen or C8-halogen help to the recognition by

Substrate:
5'-FAM-CGATCATGGAGGCTAXCGCTCCCGTTACAG-3'
3'-AGTACCTCCGATCGCGAGGGCAAT-5'
X = dG, 8-oxo-dG, 7-deazadG, 8-halogenated-7-deazadG, 8-Br-dG.

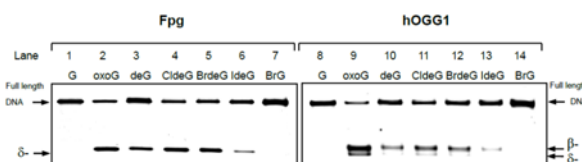


Figure 4. Glycosidase activity of 8-halogenated-7-deazadG in DNA with Fpg and hOGG1. β- and δ- indicate β elimination and δ elimination products, respectively.

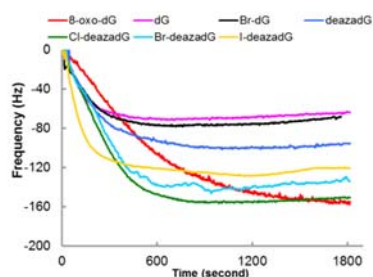


Figure 5. The time course interaction between hOGG1 and duplex DNA containing 8-oxo-dG analogues by QCM analysis.

Table 3. Kinetic parameters of duplex DNA containing 8-halogenated-7-deaza-dG derivatives for Fpg and hOGG1^a

Entry	X =	Fpg			hOGG1		
		k_{on} ($10^3 M^{-1} s^{-1}$) ^b	k_{off} ($10^{-3} s^{-1}$) ^b	K_d (nM) ^c	k_{on} ($10^3 M^{-1} s^{-1}$) ^b	k_{off} ($10^{-3} s^{-1}$) ^b	K_d (nM) ^c
1	8-oxo-dG	67.1 ± 24.8	0.78 ± 0.29	11.6 ± 2.8	70.1 ± 26.2	1.27 ± 0.47	18.1 ± 2.7
2	dG	25.6 ± 6.7	2.00 ± 0.52	78.2 ± 15	131.4 ± 26.6	3.44 ± 0.70	26.2 ± 7.0
3	Br-dG	50.9 ± 24.6	2.80 ± 1.35	55.0 ± 13	135.0 ± 47.7	3.56 ± 1.26	26.4 ± 3.6
4	deaza-dG	23.9 ± 12.0	0.54 ± 0.27	22.4 ± 5.7	97.6 ± 16.3	3.62 ± 0.60	37.1 ± 7.2
5	Cl-deaza-dG	40.6 ± 14.7	0.58 ± 0.21	14.3 ± 4.4	127.7 ± 54.2	2.44 ± 1.04	19.1 ± 4.9
6	Br-deaza-dG	42.2 ± 3.6	0.59 ± 0.05	14.0 ± 1.1	136.9 ± 46.0	2.77 ± 0.93	20.2 ± 4.6
7	I-deaza-dG	36.0 ± 13.6	1.17 ± 0.44	32.5 ± 3.1	181.9 ± 64.7	4.51 ± 1.60	24.8 ± 3.6

^a Data are means (± standard deviation) of three or more independent experiments. ^b k_{on} and k_{off} were calculated from k_{obs} and K_d . ^c K_d (the dissociation constant) were obtained by stepwise injection.

Fpg. Interestingly, the dissociation rate constants (k_{off}) for 7-deaza-dG derivatives were similar to 8-oxo-dG, implying the importance of the presence of hydrogen at 7-position. In the case of hOGG1, 8-oxo-dG exhibited much lower k_{off} value than the other compounds, probably arising from the strong hydrogen bonding between 7-NH with Gly42 in the active site of hOGG1 (Figure 6). Although 8-Cl- and 8-Br-7-deazadG had lower k_{off} value than 8-oxo-dG, they exhibited higher k_{on} which resulted in the similar dissociate constant to 8-oxo-dG. Accordingly, it has been demonstrated that 8-halogenated-7-deaza-dG containing duplexes are competitive inhibitors for the glycosidase activity of hOGG1 to excise 8-oxo-dG in duplex DNA (Figure 7).

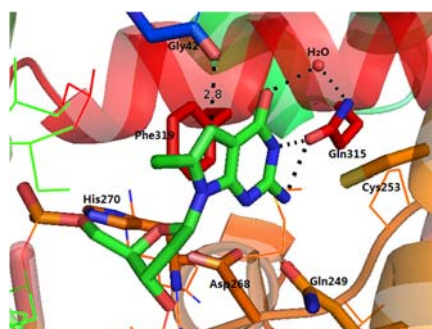


Figure 6. 8-Cl-7-deazadG in the active site of hOGG1.

Substrate (*G = 8-oxo-dG, 100 nM):
 5'-FAM-CGA TCA TGG AGG CTA *GG CTC CCG TTA CAG-3'
 3'-AGT ACC TCC GAT CGC GAG GGC AAT -5'

Competitor:
 5'- CGA TCA TGG AGG CTA *CG CTC CCG TTA CAG-3'
 3'- AGT ACC TCC GAT CGC GAG GGC AAT -5'
 X = dG, 8-oxodG, 8-BrdG, 7-deazadG and its derivatives.

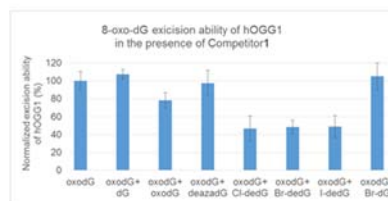
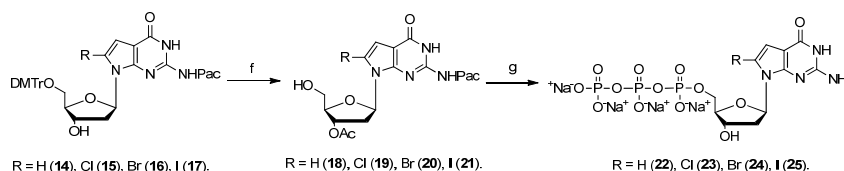


Figure 7. Bar graph of normalized excision ability of hOGG1 in the presence of corresponding 400 nM of competitor DNA (dG, 8-oxodG, deazadG, Cl-deazadG, Br-deazadG, I-deazadG and Br-dG).

3. Synthesis and evaluation of 8-halogenated-7-deaza-dGTP.

I next synthesized 7-deaza-dGTP as well as 8-Cl-, 8-Br- and 8-I-7-deaza-dGTP using the conventional method (Scheme 2). Although 8-halogenated-7-deaza-dGTP derivatives were hardly hydrolyzed by hMTH1



Scheme 2. (f) Acetic anhydride, pyridine, 61-74%; 3% trichloroacetic acid in CH_2Cl_2 , 62-84%. (g) i: 2-chloro-4H-1,3,2-benzodioxaphosphorin-4-one, pyridine/1,4-dioxane (1:1); ii: $(\text{HBU}_3\text{N}^+)_2 \text{H}_2\text{P}_2\text{O}_7^{2-}$, Bu_3N , DMF; iii: I_2 , pyridine/ H_2O (98:2); iv: 28% ammonia solution, 27-43%.

(Figure 8A), they showed competitive inhibitory activity against 8-oxo-dGTP hydrolysis by hMTH1 (Figure 8B). Docking study (Autodock 4.2.6) and molecular dynamic simulation (NAMD 2.10) revealed that 8-I-7-deazadGTP may adopt *anti*-conformation and place itself in the almost same position as 8-oxo-dGTP. However, Trp117 in the active site of hMTH1 was shifted 2 Å as compared to its position in the complex of 8-oxo-dGMP and hMTH1, which might enhance the π - π interaction between Trp117 and 8-I-7-deazadGTP (Figure 8C). Furthermore, the IC_{50} values of 8-Cl-7-deazadGTP, 8-Br-7-deazadGTP and 8-I-7-deazadGTP were determined to be 0.857, 0.496 and 0.415 μM , respectively (Table 4). And their corresponding inhibition constants (K_i) were respectively calculated to be 116.8, 78.2 and 61.7 nM by Lineweaver-Burk plots (Table 5). The diol compound of 8-I-7-deazadG exhibited some inhibitory effect against hMTH1 but it is 100-fold weaker than 8-I-7-deazadGTP, implying the importance of the triphosphate group. Interestingly, 8-halogenated-7-deazadGTP exhibited much higher inhibitory activities against hMTH1 than SCH51344 and (S)-Crizotinib. Therefore, it is expected that 7-deazadGTP and 8-halogenated-7-deazadGTP would show antitumor activity by targeting hMTH1.

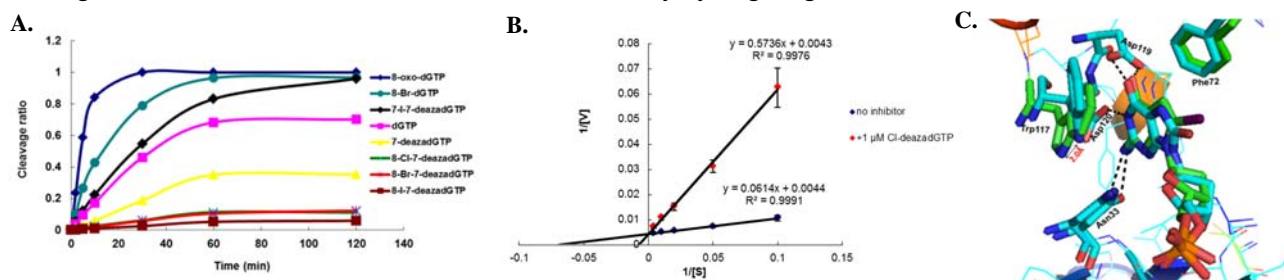


Figure 8. (A) Time course of hydrolysis of 7-deazadGTP and 8-halogenated-7-deaza-dGTP with hMTH1; (B) Lineweaver-Burk plots of 8-oxo-dGTP hydrolysis by hMTH1 in the absence of inhibitor or presence of 8-Cl-7-deazadGTP; (C) Alignment of 8-I-deazadGMP after simulation (Autodock 4.2.6 and NAMD 2.10) with 8-oxo-dGMP crystal structure (PDB: 3ZR0).

Table 4. IC₅₀ values of hMTH1 inhibitors^a

	IC ₅₀ (μM)
dGTP	1997.8±337.4
7-deazadGTP	1.57±0.12
8-Cl-7-deazadGTP	0.857±0.155
8-Br-7-deazadGTP	0.496±0.021
8-I-7-deazadGTP	0.415±0.056
8-I-7-deazadG	44.81±7.44
8-Br-dGTP	167.49±40.83
7-I-7-deazadGTP	2.62±0.12
SCH51344	2.23±0.20
(S)-Crizotinib	1.00±0.13
TH287	0.0104±0.00101

^acondition: 20 mM Tris-HCl PH 7.5, 4 mM MgCl₂, 40 mM NaCl, 80 μg/mL BSA, 8 mM DTT, 10% glycerol; 5 nM hMTH1; 50 μM 8-oxo-dGTP; various concentrations of dGTP, 7-deazadGTP, 8-halogenated-7-deazadGTP, 8-I-7-deazadG, 8-Br-dGTP, 7-I-7-deazadGTP, SCH51344, (S)-Crizotinib and TH287; 1% DMSO (for SCH51344, 8-I-7-deazadG, (S)-Crizotinib and TH287). Data are means (± standard deviation) of three or more independent experiments.

Table 5. Steady-state kinetic parameters and inhibition constants of 8-oxo-dGTP hydrolysis by hMTH1 in the absence or presence of inhibitors^a

Inhibitor	k _{cat} (S ⁻¹)	K _m (μM)	K _i (nM)
No inhibitor	18.94	13.95	
1 μM of 7-deazadGTP	17.73	79.45	213.0
1 μM of 8-Cl-7-deazadGTP	19.38	133.40	116.8
0.5 μM of 8-Br-7-deazadGTP	18.52	103.09	78.2
0.25 μM of 8-I-7-deazadGTP	17.01	70.43	61.7
3 μM of 7-I-7-deazadGTP	18.94	78.30	650.4
1 μM of SCH51344	14.12	65.78	— ^b
1 μM of (S)-Crizotinib	19.38	82.65	203.1
0.01 μM of TH287	17.01	63.33	2.83

^acondition: 20 mM Tris-HCl PH 7.5, 4 mM MgCl₂, 40 mM NaCl, 80 μg/mL BSA, 8 mM DTT, 10% glycerol; 2 nM hMTH1; 10, 20, 50, 100, 250 μM 8-oxo-dGTP; in the absence of inhibitor or in the presence of inhibitor; 37°C; 1% DMSO (for SCH51344, S-Crizotinib, or TH287); incubated for 4 min (no inhibitor) or 10 min (with inhibitor). ^bK_i for SCH51344 was not calculated.

It was found that 8-halogenated-7-deazadGTP were only slightly incorporated into DNA to pair with dC and hardly incorporated to pair with dA by KF-exo⁻ and human polymerase β (Figure 9). Moreover, 8-halogenated-7-deazadG derivatives in duplex DNA were tested to be difficult to pair with dA during replication process.

Therefore, 8-halogenated-7-deazadGTP

derivatives are expected to have little side effects, further supporting their potentials as antitumor agents.

【Conclusion】

8-Halogenated-7-deaza-dG derivatives were designed as 8-oxo-dG analogues, and their syntheses and incorporations into oligonucleotides were successful. 8-halogenated-7-deaza-dG derivatives resemble 8-oxo-dG in shape and preference for *syn*-conformation confirmed by the DFT calculations and NMR studies, but they do not form Hoogsteen base pair with the opposite dA based on the lower *T_m* values as compared to 8-oxo-dG. Interestingly, 8-halogenated-7-deaza-dG derivatives in duplex DNA, especially 8-Cl-7-deaza-dG, were good glycosidase substrates for Fpg and strong binders to hOGG1. Accordingly, 8-halogenated-7-deaza-dG derivatives in duplex DNA demonstrated competitive inhibition for the glycosidase activity of hOGG1 to excise 8-oxo-dG in duplex DNA. Furthermore, 8-halogenated-7-deazadGTP were successfully synthesized and demonstrated as strong inhibitors of hMTH1 at nanomolar concentrations. It is interesting that 8-halogenated-7-deazadGTP derivatives exhibited low mutagenic potential by DNA polymerases, implying that they might have little side effects. Thus, this study has clearly demonstrated that 8-halogenated-7-deazadG derivatives are potential to be used as probes and functional inhibitors of 8-oxo-dG repair enzymes.

【References】

- Burrows, C. J.; Muller, J. G. *Chem. Rev.*, **1998**, *98*, 1109–1152.
- Gad H.; Koolmeister T.; Jemth A.S.; Eshad S.; Jacques S.A.; Ström C.E. et al. *Nature*, **2014**, *508*, 215-221; Huber K.V.; Salah E.; Radic B.; Gridling M.; Elkins J.M.; Stukalov A.; Jemth A.S. et al. *Nature*, **2014**, *508*, 222-227.

【Publications】

- Yin, Y.; Taniguchi, Y.; Sasaki, S. Synthesis of 8-halogenated-7-deaza-2'-deoxyguanosine as an 8-oxo-2'-deoxyguanosine analogue and evaluation of its base pairing properties. *Tetrahedron*, **2014**, *70*, 2040-2047.
- Yin, Y.; Sasaki, S.; Taniguchi, Y. Recognition and excision properties of 8-Halogenated-7-deaza-2'-deoxyguanosine as 8-oxo-2'-deoxyguanosine analogue by Fpg and hOGG1. *Submitted*.

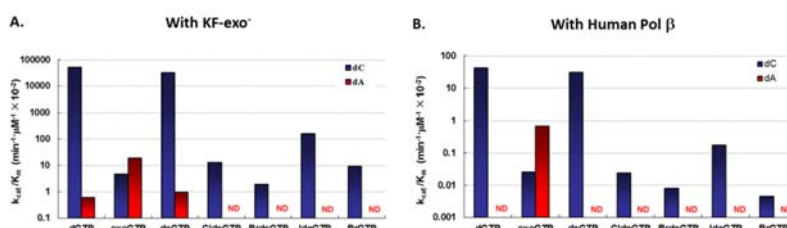


Figure 9. Incorporation of dGTP, 8-oxo-dGTP, 7-deazadGTP, 8-halogenated-7-deazadGTP and 8-Br-dGTP opposite dC, dA, dG and dT by KF-exo⁻ and Human polymerase β. A) Bar graph of incorporation efficiency (k_{cat}/K_m) with KF-exo⁻; B) Bar graph of incorporation efficiency (k_{cat}/K_m) with Human polymerase β.